
Journal of Dispersion Science and Technology

ISSN: (Print) (Online) Journal homepage: www.tandfonline.com/journals/ldis20

# Artificial neural network-based sensitivity analysis and experimental investigation of liquid–solid fluidization technique for low-grade coal upgradation

Ajita Kumari, Alok Tripathy & N. R. Mandre

JOURNAL OF DISPERSION SCIENCE AND TECHNOLOGY
2023, VOL. 44, NO. 2, 265–277
https://doi.org/10.1080/01932691.2021.1947846

# Artificial neural network-based sensitivity analysis and experimental investigation of liquid–solid fluidization technique for low-grade coal upgradation

Ajita Kumari[a,b], Alok Tripathy[c], and N. R. Mandre[a]

[a]Department of Fuel, Minerals & Metallurgical Engineering, IIT (ISM) Dhanbad, Dhanbad, India; [b]CSIR - National Metallurgical Laboratory Madras Centre, Chennai, India; [c]CSIR - Institute of Minerals and Materials Technology, Bhubaneswar, India

**ABSTRACT**

Liquid-solid fluidization technique is being applied where low-grade coal or minerals enrichment is mostly density-based. Static and dynamic behavior of particles in a fluid medium has been extensively investigated over the years because of its dynamic applications across various industries. In this work, bed characterization studies and experiments have been conducted to study coal washing ability of the liquid-solid fluidized bed separator. Results have been recorded in terms of ash rejection%, combustible recovery% and separation efficiency%. Minimum fluidization velocity and pressure drop values have been predicted using existing theoretical correlations and compared with the experimental values. A three-layered (4:5:3) feedforward back-propagation (FFBP) neural network model was developed using Levenberg-Marquardt algorithm, LOGSIG and MSE as training, transfer and performance functions respectively. Garson's algorithm and connection weight approach have been employed for sensitivity analysis to interpret the neural network results physically. Coefficients of correlation, all R (including training, validation & testing datasets) obtained for outputs ash rejection ($R = 0.9960$), combustible recovery ($R = 0.9952$) and separation efficiency ($R = 0.9944$) suggest that predicted values are in agreement with the experimental values and the developed model is a good fit.

**ARTICLE HISTORY**
Received 2 February 2021
Accepted 12 June 2021

**KEYWORDS**
Liquid-solid fluidized bed separator; bed characterization studies; artificial neural network; Levenberg-Marquardt algorithm; sensitivity analysis

**GRAPHICAL ABSTRACT**

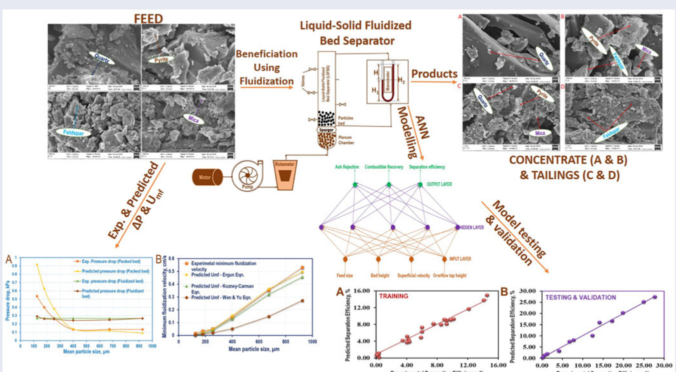


## Introduction

Coal is responsible for fueling a significant part of world electricity. Despite increasing usage of hydro, nuclear, oil, gas and renewables, coal is still the fastest-growing energy source in recent years. Mining of deeper seams is increasing the ash content in the coal produced. Inherent ash is much more in Indian coal (owing to its drift origin) as compared to the extraneous ash and therefore calls for special technologies of fine coal washing. Increasing import of low ash coal is affecting the national economy. Indian coal contains high amount of impurities and substantial near gravity materials (NGM) and needs to be beneficiated before being used for coke making.[1–5] Because of poor liberation at coarse sizes, beneficiation of coal fines is necessary to achieve high cleanability, better productivity and environmental compliability.[6]

Converting static state of solid particles to dynamic fluid-like state by an upward flowing fluid is known as fluidization. The bed remains static at fluid velocities lesser than minimum fluidization velocity ($U_{mf}$) and with higher velocities, the bed starts to fluidize and an interface develops

CONTACT Ajita Kumari akajitakumari@gmail.com Department of Fuel, Minerals & Metallurgical Engineering, IIT (ISM) Dhanbad, Dhanbad, India.
Supplemental data for this article can be accessed online at https://doi.org/10.1080/01932691.2021.1947846.

Table 1. Range of input parameters for bed characterization & experiments.

| Input parameters | Range/values |
|---|---|
| Feed size, μm | −1000 + 850 (925), −850 + 500 (675), −500 + 300 (400), −300 + 210 (255), −210 + 150 (180), −150 + 100 (125) |
| Bed height, cm | 10, 20, 30 |
| Superficial velocity, cm/s | 0.35, 0.71, 1.06, 1.41, 1.77, 2.12, 2.48, 2.83, 3.18, 3.54 |
| Overflow tap height, cm | 12, 37, 62 |

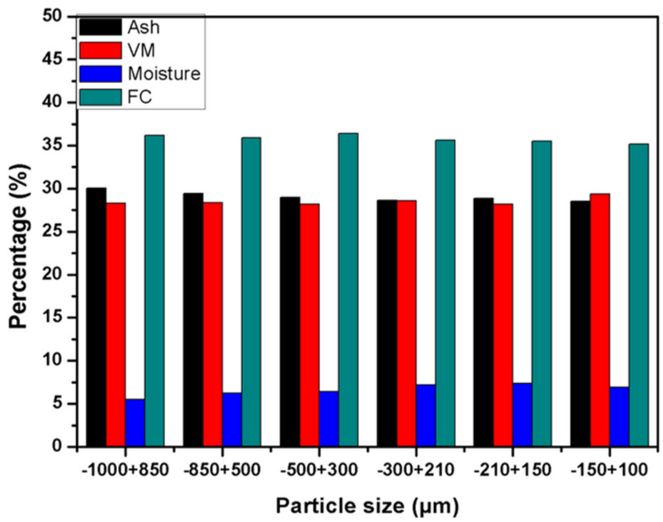


Figure 1. Proximate analysis of coal feed sample.

inside the fluidization column.[7–10] Mixing and segregation properties of fluidized bed separators can be exploited for many industrial processes but are of particular significance for mineral and coal separations, where a small amount of valuable matter is mixed with a large number of gangue particles. Multi-variant nature of minerals and ores require ore-specific fluidization conditions for processing. Physical properties of the mineral particles, properties of packed/fluidized beds and superficial fluid (water, in this case) velocity are major operating parameters in liquid-solid fluidization operation.[11,12] The minimum fluidization velocity is a characteristic property of fluidized beds, marking a change of a packed bed to fluidized state.[13–17] Beneficiation studies by gas-solid fluidization route has been reported by many authors.[18–21] Kumari et al.[12] reported process efficiency and misplacement studies on liquid-solid fluidization for coal beneficiation, using statistical optimization method. The present study focuses on predicting the effect of bed height, overflow tap height, superficial velocity and feed size on the beneficiation of low-grade coal particles in a liquid-solid fluidized bed separator using artificial neural network. The performance has been judged by outputs such as ash rejection, combustible recovery and separation efficiency. Pressure drop and bed expansion profiles have been studied with change in superficial velocity. Experimental and predicted values (using existing verified correlations) of minimum fluidization velocity, $U_{mf}$ and pressure drop, $\Delta P$ have been compared in this work.

Neural network modeling and sensitivity analysis are being used for solving prediction, regression and classification problems in various engineering fields.[22–26] The main objective the present work is to develop an ANN based model, which would help in developing the control mechanism for plant operators. The industrial use of liquid solid fluidization is increasing steadily in the mineral beneficiation industries especially in coal washing. The present paper aims at developing an artificial neural network model which would provide opportunities for the plant operators to control the operating parameters in a more precise manner for Indian high ash non-coking coal.

ANN modeling of liquid-solid fluidization of natural ores and coal are very limited or not available for Indian coal washing. Indian coal has a unique characteristic of high near gravity materials (NGM) and the mineral materials are well distributed in the coal matrix. Hence, it is essential to develop unique ANN model for Indian coal. In this work, an ANN model was developed to determine the output values computationally. A feed forward back-propagation (FFBP) three-layered (4:5:3) neural network was designed to model, predict and analyze the fluidization process of coal beneficiation. The ANN model was trained to achieve the target values with minimal errors, using Levenberg-Marquardt (LM) algorithm.[27,28] The model was optimized by re-training and minimizing of errors using back propagation (mean square error) method. The predictability of the ANN model has been estimated with respective R values (coefficient of correlation). Sensitivity analysis of input parameters has also been carried out using Garson's algorithm and connection weight approach. The order of relative contribution of the input parameters for different outputs has been presented as ranking.

## Materials and methods

### Sample preparation

ROM non-coking coal was collected from Rajmahal coalfield region in Jharkhand. ROM sample, as received, was first mixed thoroughly by repeated hip and reclaiming processes, then cone and quartering method was applied to generate the represented sample for the study. This sample was crushed and size analyzed into different size fractions: $-1000+850\,\mu$m, $-850+500\,\mu$m, $-500+300\,\mu$m, $-300+210\,\mu$m, $-210+150\,\mu$m and $-150+100\,\mu$m. Coning and quartering method was used to draw out representative samples for proximate and other characterization analyses. Bed characterization and beneficiation studies of the six size-fractions were carried out under different ranges of input parameters mentioned in Table 1.

### Characterization studies

An air-dried based proximate analysis of the six size-fractions was carried out, as presented in Figure 1, for comparison and interpretation.

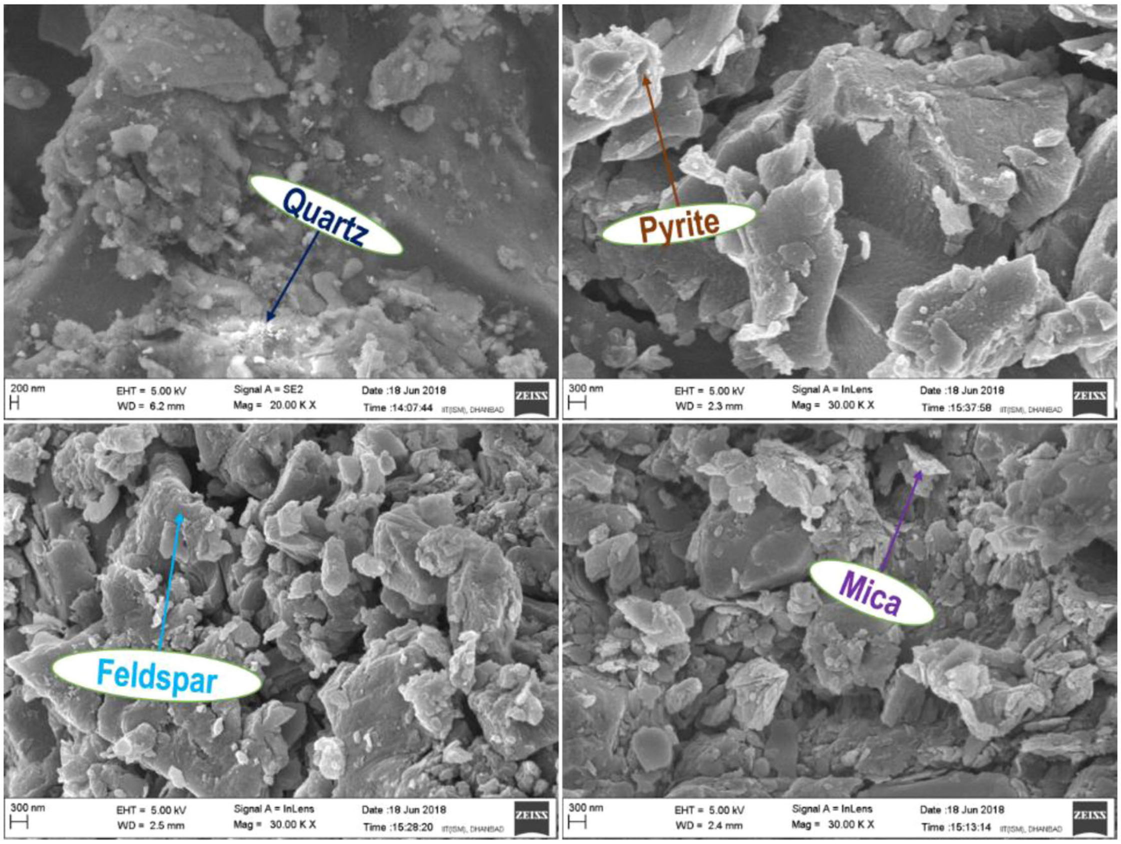


**Figure 2.** SEM images of coal feed sample.

Proximate analysis of some size-fractions were carried out by the authors in their earlier work and reported in a paper.[12] Mineralogical characterization studies of the coal sample of size $-1000+850\,\mu$m have been done by SEM, XRD and petrographic analyses.

Scanning Electron Microscopy (SEM) evaluation of the coal feed particles was performed, using a FEI 430 Nova Nano-SEM model JXA8230, while maintaining the acceleration tension at 5 kV.

The images of the SEM (Figure 2) show a large black area, which indicates opaque and lustrous carbonaceous matter. Light-brass grains indicate the presence of pyrite ($FeS_2$) and plate-like structure indicates feldspar (aluminium silicates, $KAlSi_3O_8$) presence. It also shows the hematite matter associated with alumina and quartz particles and porous fractures, filled with organic matter.

## Experimental

**Figure 3** illustrates the working of the experimental setup.[29] A 1.5 m high and 0.1 m wide cylindrical column made of glass was used for the fluidization studies. Different rotameters, having various ranges were installed to ascertain controlled flow and to maintain a pre-set flowrate of water in an upward direction. U-tube mercury manometer was used to measure the pressure drop across the fluidization column.

The change in bed height was observed and noted manually. The different overflow tapping heights are at 12, 37, 62, 87 and 112 cm, which were used for sample collection. Experiments were conducted by changing the feed size, bed height, superficial velocity and overflow tap height, as per Table 1. Some of the data used in the present study has been taken from the earlier published work of the authors for comparison and interpretation for large range of input parameters.[12]

## Artificial neural network (ANN) modeling

Artificial neural network is a mathematical tool for prediction of output or responses using learning algorithm and used for parallel-processing capabilities via modeling. It uses a set of algorithms, designed to recognize patterns and create mapping between noisy set of input and output data and then, predict data interactions. Outputs are calculated, using a linear combination using its input weights and passing the output through a non-linear transfer function.[24,25,30]

$$Y = f\{(W * X) + B)\} \tag{1}$$

where, Y is output, X is input, W are weights, B is offset bias and f is the transfer function.

The Levenberg-Marquardt (LM) algorithm is a technique for detection of function's minima using second-order training speed. It is a combination of gradient descent and Gauss-Newton methods. Gradient descent method determines the minima of a least square error function, using a first-order iterative optimization whereas, in Gauss-Newton method, the error is reduced by finding the minima of the

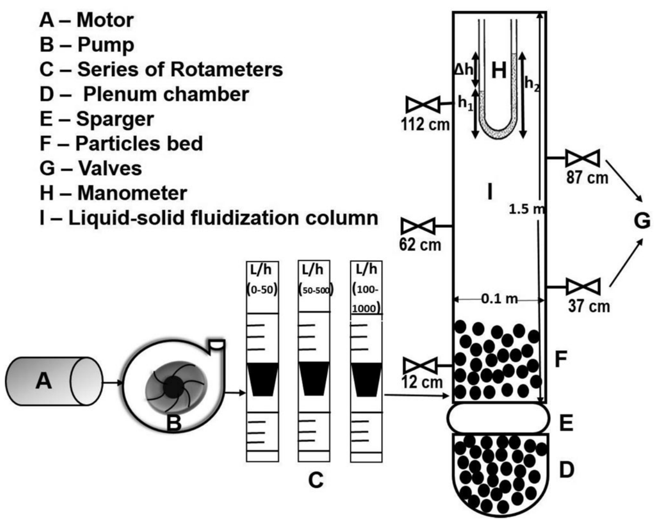


Figure 3. Schematic diagram of experimental set-up.

least square function which is assumedly quadratic.[27,28] Back-propagation methods calculate the function gradient with respect to all the weights of the network and to minimize the prediction errors in order to determine optimal values of weights.[26,31,32] Error is calculated in terms of mean square error (MSE) and mean absolute percentage error (MAPE). MSE is the squared average difference between target data and the data estimated. MAPE is the average absolute percentage error, which is used to check the efficiency of prediction. These errors can be calculated using the formulae:

$$\mathrm{MSE} = \frac{1}{N}\sum_{i=1}^{N}\left(Y_i - \hat{Y}_i\right)^2 \tag{2}$$

$$\mathrm{MAPE} = 100 * \frac{1}{N} * \sum_{i=1}^{N}\left|\frac{\left(Y_i - \hat{Y}_i\right)}{\left(Y_i\right)}\right| \tag{3}$$

Where, N is total training samples, MSE is the error of network for a single iteration, MAPE is the average percentage error, $Y_i$ is targeted value and $\hat{Y}_i$ is output value. Coefficient of correlation (R) is a statistical measure of degree of relationship between two variables and can vary in the range $-1$ to 1. It can be expressed as [www.statisticshowto.com]:

$$R = \frac{N(\sum XY) - (\sum X)(\sum Y)}{\sqrt{[N\sum X^2 - (\sum X)^2][N\sum Y^2 - (\sum Y)^2]}} \tag{4}$$

Coefficient of correlation value $-1$ represents a strong negative relationship and $+1$ represents a strong positive relationship between the data points. R values further away from 0 and closer to $+1$ show that the model establishes a strong relationship between dataset and is highly efficient for the given process. NN toolbox available in MATLAB R-2014A (trial version) was employed to carry out the computational studies.

### *Sensitivity analysis*

Sensitivity analysis is carried out to identify the critical parameters and their proportional contribution to the outputs. There are different sensitivity analysis methods suggested for the determination of order of significance of the input parameters on the outputs: A) Partial derivative (PaD) method, B) Profile method, C) Stepwise method, D) Connection weight approach (CWA) and E) Garson's algorithm (GA). Connection weight approach calculates the product of all the connection weights (raw values) between each input and output neuron and sums the products across all the hidden neurons. Garson's algorithm, also known as weights method, utilizes absolute values of weights associated with each input neuron. The main issue with Garson's algorithm is that it fails to account for the different influences of weights because this method uses the absolute values of connection weights, whereas the main problem with connection weight approach that during summation, positive and negative connection weights can cancel their contribution which leads to inconsistent results.[33–36]

## Results and discussion

### *Bed characterization studies*

For a given feed size, bed height and superficial fluid velocity, bed characterization or hydrodynamics studies determine how the sample will behave inside the fluidization column. Kumari et al.[12] has discussed the pressure drop and bed expansion profiles of the three size-fractions under study. **Figures 4–6** show the pressure drop and expanded bed profile of other three size-fractions also at different bed heights.

It was observed that with increase in static bed height, the pressure drop is increasing. Once the bed gets fluidized, the pressure drop remains unchanged. On the contrary, the height of packed bed is constant and starts increasing, only after fluidization. Bed height expansion, following the same pattern as that of pressure drop, shows increment in bed height with increasing superficial velocity (after attainment of fluidization). The velocity-ranges were observed for packed and fluidized beds for all size-ranges and bed heights to study the fluidization behavior. Figures 4–6 show the pressure drop and bed expansion profiles of all particle size-fractions at static bed heights of 10, 20 and 30 cm to understand the effect of particle size on the hydrodynamics of the fluidized bed. Data for plotting pressure drop curve and bed expansion of three size fractions (i.e., $-1000+850\,\mu$m, $-850+500\,\mu$m, $-500+300\,\mu$m) out of six size-fractions were taken from the authors' previous work.[12] From the figures, it can be observed that with the increase in particle size, the pressure drop increases and bed expansion decreases. This phenomenon happens because when particle size increases, the force required to fluidize the particle increases and it becomes more difficult for bed to expand at the same input force. Another important observation from the Figures 4–6 is that, during the packed bed condition, the increase of pressure drop is not a smooth line curve having uniform slope. Instead, the pressure drop curves have

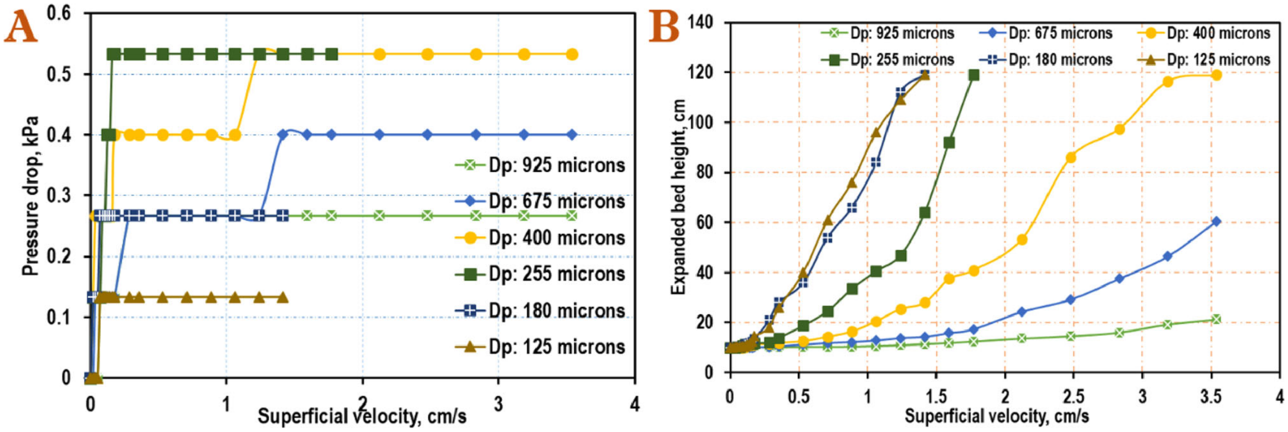


Figure 4. Pressure drop (A) and bed expansion (B) profiles of coal particles of various sizes at bed height of 10 cm.

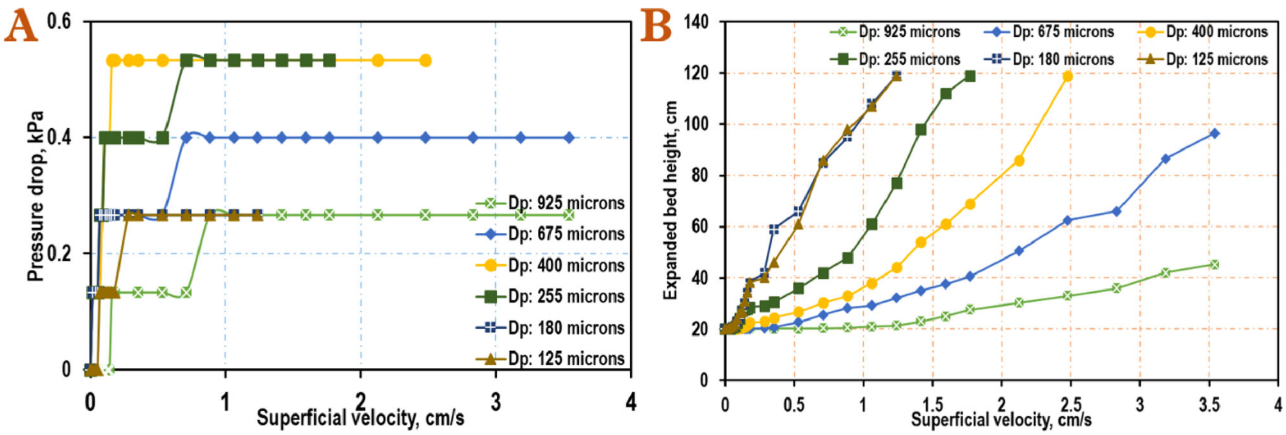


Figure 5. Pressure drop (A) and bed expansion (B) profiles of coal particles of various sizes at bed height of 20 cm.

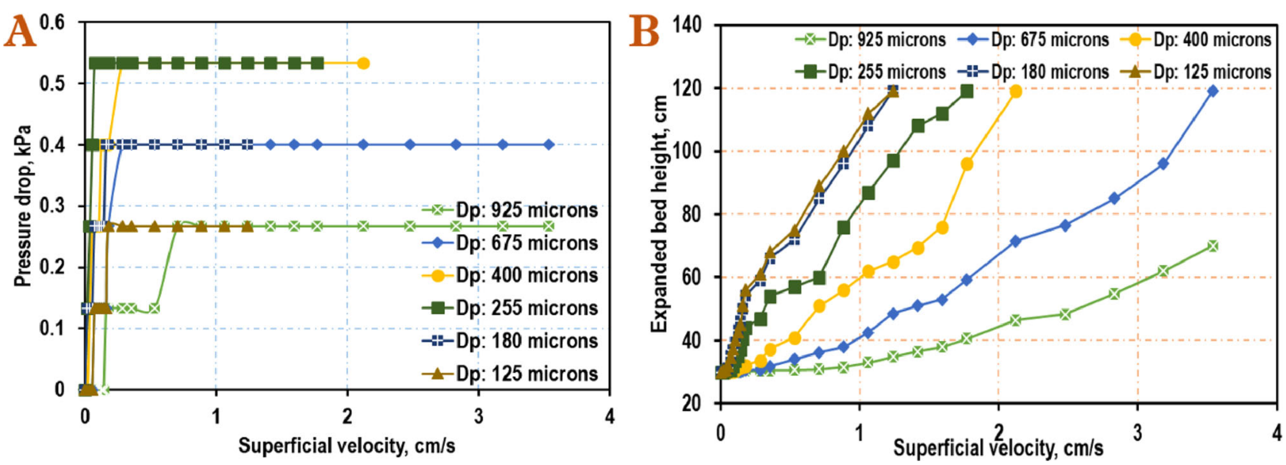


Figure 6. Pressure drop (A) and bed expansion (B) profiles of coal particles of various sizes at bed height of 30 cm.

variable slope in the static bed region. This phenomenon happens because the coal particles are not of mono-size, mono-density nature; they have a particle size distribution even in close size-ranges.[13,37]

## Estimation of pressure drop and minimum fluidization velocity

Pressure drop across any column can be given as:

$$\Delta P = (\rho_p - \rho_f).(1 - \varepsilon).g.H \tag{5}$$

Here, $\rho_p$ is particle density, $\rho_f$ is fluid density, H is bed height.

Ergun proposed an equation explaining the friction and total energy loss inside a packed bed,[38] which can be rearranged as:

$$\frac{\Delta P}{L} = 150\,\frac{(1-\varepsilon)^2}{\varepsilon^3}\frac{\mu}{{d_p}^2}.U + 1.75\frac{(1-\varepsilon)}{\varepsilon^3}\frac{\rho_f}{d_p}.U2 \tag{6}$$

Pressure drop values have been predicted for fluidized and packed beds using equations (5) and (6) respectively.

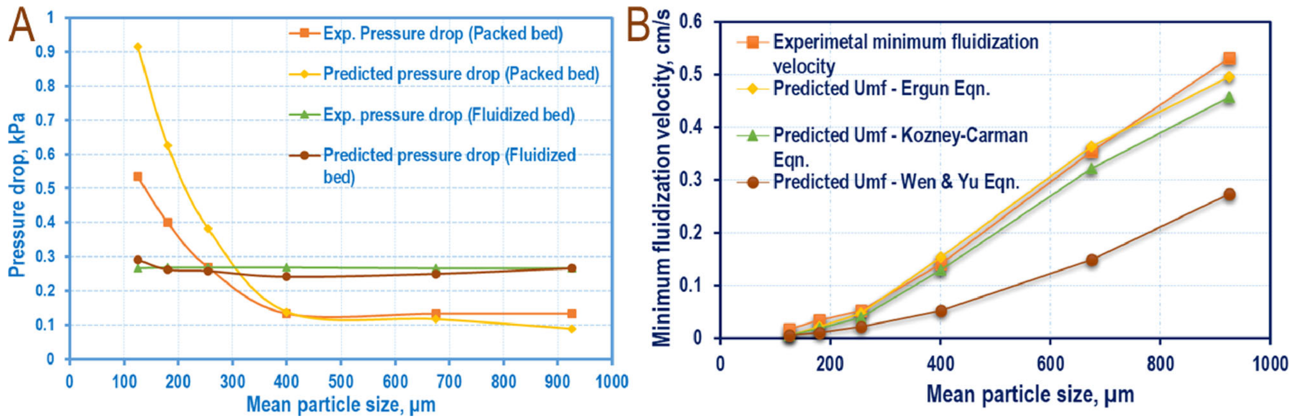


**Figure 7.** Experimental vs. predicted pressure drop (A) of packed and fluidized beds and minimum fluidization velocity (B) for different feed sizes.

Pressure drop values for packed bed were calculated at superficial velocity of 0.35 cm/s, bed height of 10 cm and feed size-ranges of $-1000+850\,\mu$m, $-850+500\,\mu$m, $-500+300\,\mu$m, $-300+210\,\mu$m, $-210+150\,\mu$m and $-150+100\,\mu$m. Experimental values for pressure drop at the above mentioned experimental conditions are 0.1334, 0.1334, 0.1334, 0.2688, 0.4002 and 0.5336 kPa for all six size-fractions respectively. Equation (5) is applied for the fluidized bed and Equation (6) is applied for packed bed conditions. These values have been compared with the experimental pressure drop values and presented in **Figure 7A**. It shows that the experimental values are close to the predicted values. The given arrangement of Ergun equation (Equation 6) shows its resemblance with the Kozney-Carmen equation which is used for pressure drop calculation of a fluid flowing in a laminar fashion via packed bed.[39] The equation is given as:

$$\frac{\Delta P}{L} = \frac{-180\mu}{\varphi_s^{2} d_p^{2}} \frac{(1 - \varepsilon)^2}{\varepsilon^3}\, Us \qquad (7)$$

This equation relates the permeability of fluidization bed, packed with solids to inter-particle porosity (1-$\varepsilon$ ), bed morphology ($\varepsilon$ ) and particle size ($d_p$) and shape ($\varphi$). Another equation proposed to determine minimum fluidization velocity was by Wen & Yu,[40] which is

$$Umf = \frac{\mu}{\rho_f d_p}\left(\left(\sqrt{1135.7 + 0.0408\ Ar}\right) - 33.7\right) \qquad (8)$$

Minimum fluidization velocity values were calculated using the above mentioned formulae (Equations 6, 7 & 8).

**Figure 7B** shows the comparison of experimental and predicted values of minimum fluidization velocity. The values predicted using Ergun equation were found nearest to that of the experimental values.

### *Effect of operating parameters on the outputs*

The effect of different operating parameters has been individually studied to observe the coal fluidization behavior, under various experimental conditions. The parameters under study are a) feed size, b) overflow tap height, c) bed height and d) superficial velocity. Ash rejection% and combustible recovery% have been calculated, using the equations given below:[41]

$$\text{Ash rejection\% in clean coal} = 100 - \frac{Y_c A_c}{A_f} \qquad (9)$$

$$\text{Combustible recovery\% in clean coal} = \frac{Y_c(100 - A_c)}{(100 - A_f)} \qquad (10)$$

Separation efficiency indicates the fluidized bed separator performance and efficiency of the separation process. Separation efficiency% has been calculated, using the formula:

$$\text{Separation efficiency (\%)} = \frac{Y_c(100 - A_c)}{(100 - A_f)} - \frac{Y_c A_c}{A_f} \qquad (11)$$

where $Y_c$ is clean coal yield%, $A_c$ is clean coal ash% and $A_f$ is feed ash%.

### *Effects of bed height & overflow tap height*

At 2.12 cm/s superficial velocity, 37 cm overflow tap height and feed size of $-850+500\,\mu$m, effect of bed height at 10, 20 and 30 cm on ash rejection% and combustible recovery% were studied. Effect of process efficiency was also studied at 2.12 cm/s superficial velocity; 62 cm overflow tap height and feed size of $-500+300\,\mu$m. With an increase in static bed height from 10 to 20 cm, ash rejection% decreases and then increases when bed height increases from 20 to 30 cm; as can be seen from **Figure 8A**. With the increase in static bed height, the amount of coal sample increases suggesting that a particular superficial velocity is required to fluidize particles of certain size, density (weight) and shape. At the given velocity, optimum result of separation efficiency 8.94% in case of feed size $-850+500\,\mu$m and separation efficiency of 14.09% in case of feed size $-500+300\,\mu$m were obtained at the bed height of 20 cm.

Effect of overflow tap height (12, 37 and 62 cm) was studied by maintaining the bed height at 10 cm, superficial velocity at 2.12 cm/s and feed size-range at $-850+500\,\mu$m and $-500+300\,\mu$m respectively. This set of experiments was mainly done to observe the dilation features of the particle bed. It can be seen from **Figure 8B** that with increase in overflow tap height, ash rejection% increases. But the least combustible recovery% was obtained at upper overflow

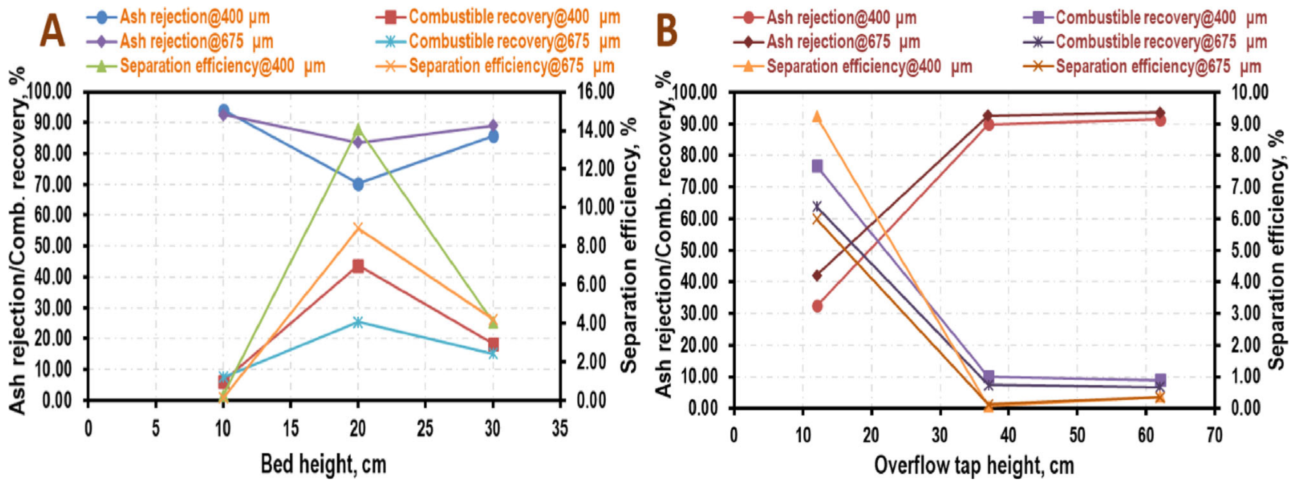


Figure 8. Effect of A) bed height and B) overflow tap height on ash rejection, combustible recovery and separation efficiency.

tap height (62 cm). In case of bed height 10 cm, the beds were dilated only upto 17 cm in case of feed size-range of $-850 + 500\,\mu$m and $-500 + 300\,\mu$m (based on bed characterization studies). So, concentrates obtained at higher overflow tapping heights don't show good carbonaceous matter recovery as suspended particles don't fluidize beyond a certain height at a given superficial velocity. Further, with increase of overflow tap height at any particular operational superficial velocity, the bulk density of the particle bed decreases. This reduces the yield and ultimately the combustible recovery. Optimum separation efficiencies of 5.89% and 9.24% were obtained in case of feed size-range of $-850 + 500\,\mu$m and $-500 + 300\,\mu$m respectively.

### Effects of feed size and superficial velocity

Maintaining the bed height, superficial velocity and overflow tap height constant at 10 cm, 2.12 cm/s and 12 cm respectively, the effect of feed size (-1000 + 850, $-850 + 500$, $-500 + 300$, $-300 + 210$, $-210 + 150$, $-150 + 100\,\mu$m) on the process efficiency was investigated. The results shown in **Figure 9A** indicate that ash rejection% is highest at coarsest feed size i.e., $-1000 + 850\,\mu$m with very low combustible recovery%, which may be due to the reason that the larger particles requiring higher superficial velocity to fluidize and segregate. At the same velocity in case of finer feed, finer gangue particles also can report to the upper zone of the column along with carbonaceous materials, resulting in high combustible recovery% but lesser ash rejection%. Highest separation efficiency of 10.14% was obtained feed size $-300 + 210\,\mu$m with ash rejection of 93.81%.

While maintaining the bed height at 10 cm, overflow tap height at 12 cm and feed size of $-1000 + 850\,\mu$m, the effect of superficial velocity (0.35, 0.71, 1.06, 1.41, 1.77, 2.12, 2.48, 2.83, 3.18 and 3.54 cm/s) was studied and the results are reported in **Figure 9B**. From the results, it was observed that an increase in superficial water velocity results in the consistent increase in combustible recovery%, with simultaneous decrease in ash rejection%. Thus, selecting an appropriate superficial fluid velocity is very crucial for achieving an optimum output. At superficial velocity of 3.54 cm/s, separation efficiency was observed to be the highest (27.71%), in the set of experimental conditions maintained for the present study. This set of experimental condition was noted as the best for achieving the maximum separation efficiency, which suggests highest process performance.

**Figure 10** shows the SEM images of the concentrate and tailing obtained at experimental conditions of feed size-range of $-1000 + 850\,\mu$m, bed height of 10 cm, superficial velocity of 3.54 cm/s and overflow tap height of 12 cm. It can be seen that the concentrates show enhanced carbonaceous matter to that of the coal feed sample, confirming coal cleaning and gangue separation inside the fluidization column.

### Pre-processing and modeling of FFBP neural network

Generalization is the ability to handle the unseen and unorganized data and ANN models should have good generalization ability to improve the network efficiency. Neural networks are capable of auto-generalization. In the process of modeling, initiated by training method (Levenberg–Marquardt algorithm), random and noisy input dataset is classified into significant outputs and arranged in a meaningful pattern. Moreover, before training the input dataset using Levenberg–Marquardt algorithm ("trainlm"), Bayesian regularization ("trainbr") method was applied for regularization and generalization of the input dataset. This function is also available in "neural fitting tool (nftool)" section.

Liquid solid fluidization processes are very complex unit operations, which depends on the number of operating parameters. Further, the heterogeneous characteristics of coal adds to the complexity of the problem. In addition to this, most of the time outputs dependency on the input parameters are nonlinear in nature. Furthermore, a few thumb rules are generally being used to choose number of nodes/neurons for the hidden layer. There are many rules-of-thumb for determining an acceptable number of neurons to use in the hidden layers, such as the following [Source: https://www.heatonresearch.com/2017/06/01/hidden-layers.html]:

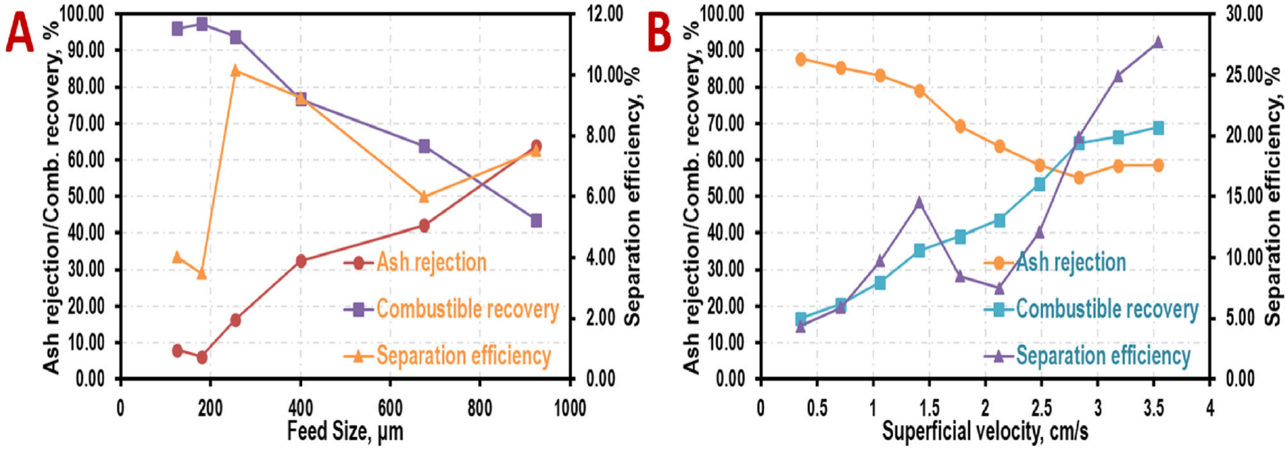


**Figure 9.** Effect of (A) feed size and (B) superficial velocity on ash rejection, combustible recovery and separation efficiency.

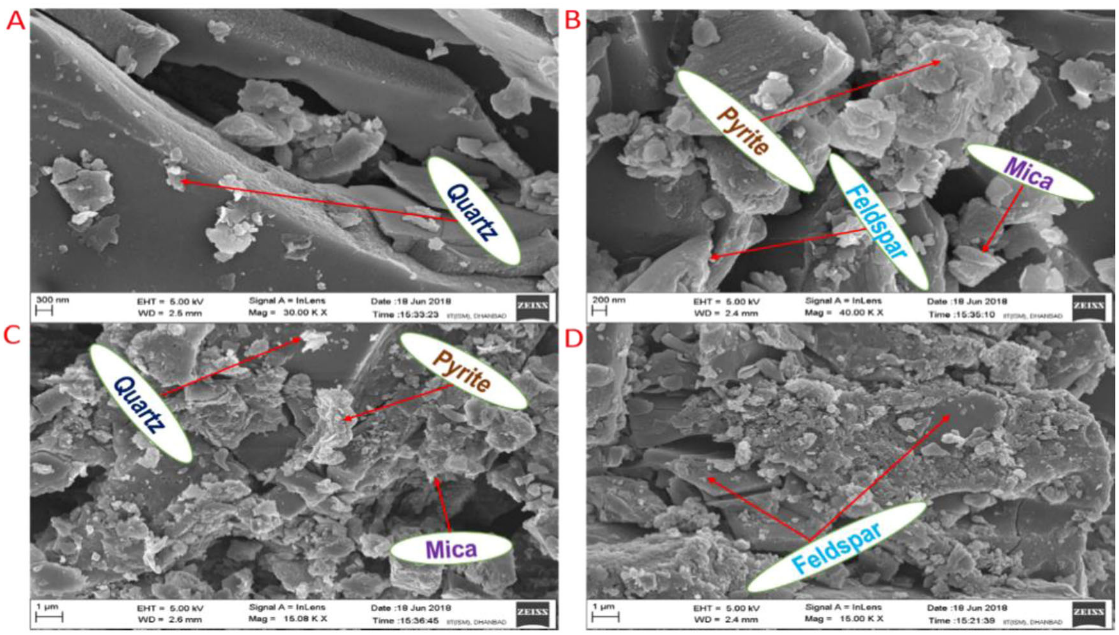


**Figure 10.** SEM images of coal concentrates (A&B) and tailings (C&D) at feed size-range of -1000 + 850 $\mu$m, bed height of 10 cm, superficial velocity of 3.54 cm/s & overflow tap height of 12 cm.

- The number of hidden neurons should be 2/3 the size of the input layer, plus the size of the output layer.
- The number of hidden neurons should be less than twice the size of the input layer.

Using these rules as starting point for neural architecture formation and finalizing the optimal number of neurons for hidden layer through trial and error. Different architectures were tried for training the network (based on the previous literature data for other mineral processing systems) using the software. The architecture which has given the least error (MAPE/MSE) values or maximum R values was selected for ANN modeling. Hence, a three-layered ANN architecture having one hidden layer was found most suitable for handling such complex system.[24,42] A three-layered (4:5:3) FFBP neural network, for modeling the liquid-solid fluidization system, has been presented in **Figure 11**.

Four nodes of first (input) layer represent feed size, bed height, superficial velocity and overflow tap height; middle layer has five nodes (black box containing activation function) and three nodes of last (output) layer indicate ash rejection, combustible recovery and separation efficiency. Output values can be predicted using the developed model by feeding new input dataset of the process. 70% data have been used for training and 30% for verification and testing purposes. The network specifications have been mentioned in **Table ST1** (supplementary file). Network specifications are: Levenberg-Marquardt algorithm as training function; MAPE and MSE as performance function; learning rate as 0.10; momentum coefficient as 0.40; Logarithmic sigmoid function (LOGSIG) as transfer/activation function; number of iterations as 1000 and epoch as 65. **Table 2** shows the entire 37 datasets used in modeling of the system.

Some data points have been collected from the previously published work of the authors.[12] Backpropagation algorithm was applied to the dataset, in an iterative manner, to obtain minima of error function. Transfer function LOGSIG

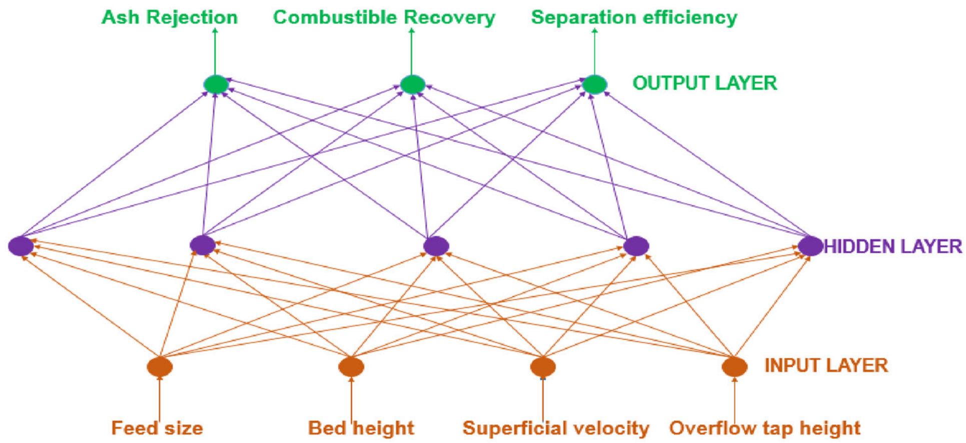


**Figure 11.** Artificial neural network (ANN) scheme.

**Table 2.** Experimental data set.

| Run No. | Feed size-range, μm | Mean particle size, μm | Bed height, cm | Superficial velocity, cm/s | Overflow tap height, cm |
|---|---|---|---|---|---|
| 1 | −1000 + 850 | 925 | 10 | 2.12 | 12 |
| 2 | −850 + 500 | 675 | 10 | 2.12 | 12 |
| 3 | −500 + 300 | 400 | 10 | 2.12 | 12 |
| 4 | −300 + 210 | 255 | 10 | 2.12 | 12 |
| 5 | −210 + 150 | 180 | 10 | 2.12 | 12 |
| 6 | −150 + 100 | 125 | 10 | 2.12 | 12 |
| 7 | −500 + 300 | 400 | 10 | 2.12 | 12 |
| 8 | −500 + 300 | 400 | 10 | 2.12 | 12 |
| 9 | −500 + 300 | 400 | 10 | 2.12 | 12 |
| 10 | −850 + 500 | 675 | 10 | 2.12 | 12 |
| 11 | −850 + 500 | 675 | 10 | 2.12 | 37 |
| 12 | −850 + 500 | 675 | 10 | 2.12 | 62 |
| 13 | −500 + 300 | 400 | 10 | 2.12 | 62 |
| 14 | −500 + 300 | 400 | 20 | 2.12 | 62 |
| 15 | −500 + 300 | 400 | 30 | 2.12 | 62 |
| 16 | −850 + 500 | 675 | 10 | 2.12 | 37 |
| 17 | −850 + 500 | 675 | 20 | 2.12 | 37 |
| 18 | −850 + 500 | 675 | 30 | 2.12 | 37 |
| 19 | −1000 + 850 | 925 | 10 | 0.35 | 12 |
| 20 | −1000 + 850 | 925 | 10 | 0.71 | 12 |
| 21 | −1000 + 850 | 925 | 10 | 1.06 | 12 |
| 22 | −1000 + 850 | 925 | 10 | 1.41 | 12 |
| 23 | −1000 + 850 | 925 | 10 | 1.77 | 12 |
| 24 | −1000 + 850 | 925 | 10 | 2.12 | 12 |
| 25 | −1000 + 850 | 925 | 10 | 2.48 | 12 |
| 26 | −1000 + 850 | 925 | 10 | 2.83 | 12 |
| 27 | −1000 + 850 | 925 | 10 | 3.18 | 12 |
| 28 | −1000 + 850 | 925 | 10 | 3.54 | 12 |
| 29 | −1000 + 850 | 925 | 10 | 2.12 | 12 |
| 30 | −1000 + 850 | 925 | 20 | 2.48 | 37 |
| 31 | −1000 + 850 | 925 | 30 | 2.83 | 62 |
| 32 | −850 + 500 | 675 | 10 | 2.48 | 62 |
| 33 | −850 + 500 | 675 | 20 | 2.83 | 12 |
| 34 | −850 + 500 | 675 | 30 | 2.12 | 37 |
| 35 | −500 + 300 | 400 | 10 | 2.83 | 37 |
| 36 | −500 + 300 | 400 | 20 | 2.12 | 62 |
| 37 | −500 + 300 | 400 | 30 | 2.48 | 12 |

**Table 3.** Weights and biases for the input-hidden and hidden-output layers.

| | | Neurons in the hidden layer | | | | |
|---|---|---|---|---|---|---|
| Inputs/Outputs | Initial bias ($b_0$) | Neuron 1 | Neuron 2 | Neuron 3 | Neuron 4 | Neuron 5 |
| A: Feed size | – | −0.2279 | −1.1846 | 0.047 | 1.0447 | 1.1532 |
| B: Bed height | – | −0.9552 | −0.9183 | 0.3168 | 0.4153 | −0.2559 |
| C: Superficial velocity | – | −1.2226 | 1.411 | −2.0374 | −1.1669 | −1.104 |
| D: Overflow tap height | – | −1.3869 | 0.381 | 0.3593 | −1.3256 | 1.3299 |
| $Bias_{hidden\text{-}output}$ | – | 2.0935 | 1.0467 | 0.5648 | 1.1319 | 2.2125 |
| Ash rejection | 1.6215 | 0.5004 | −0.7888 | 0.7855 | −0.7056 | −1.0267 |
| Combustible recovery | 0.7914 | 0.5698 | 1.0407 | 0.6841 | −0.2429 | 1.0521 |
| Separation efficiency | −1.744 | 0.9839 | 1.0916 | 0.0301 | −0.8249 | −0.4477 |

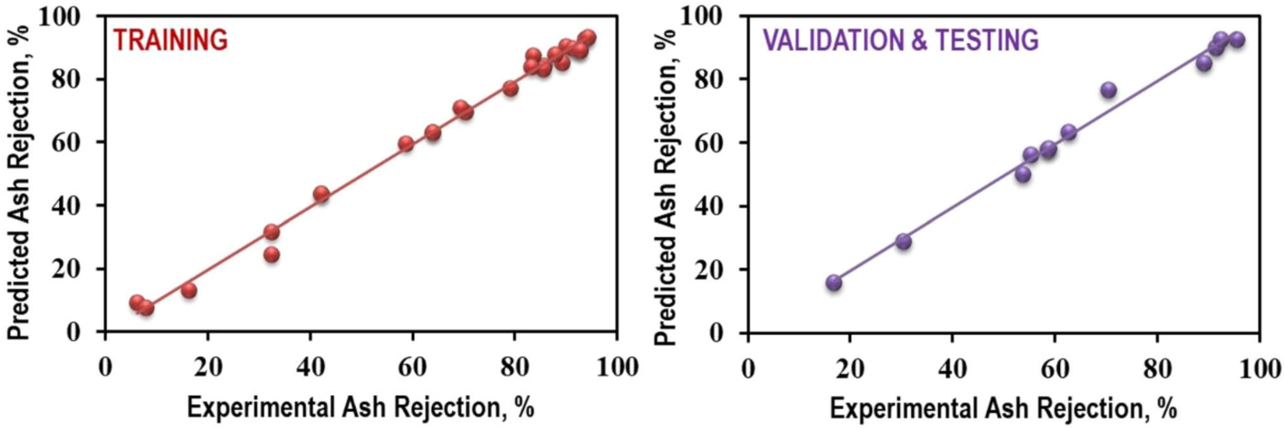


**Figure 12.** Experimental vs. ANN-predicted values of training, validation & testing datasets for ash rejection.

**Table 4.** MAPE, MSE and R values for training, validation and testing sets.

| | Training | | | Validation | | | Testing | | |
|---|---|---|---|---|---|---|---|---|---|
| Responses | MAPE | MSE | R | MAPE | MSE | R | MAPE | MSE | R |
| Dataset used | | 25 | | | 6 | | | 6 | |
| Ash rejection | 5.6302 | 1.542 | 0.9961 | 1.0816 | 0.6166 | 0.9988 | 5.1850 | 2.9433 | 0.9927 |
| Combustible recovery | 10.4349 | 0.2869 | 0.9952 | 4.8567 | 0.0957 | 0.9988 | 11.5141 | 1.5095 | 0.9983 |
| Separation efficiency | 9.3342 | 0.7027 | 0.9867 | 5.9821 | 2.1879 | 0.9996 | 6.8117 | 1.6778 | 0.9798 |

(Log-Sigmoid) is represented by the equation below [www.mathworks.com]:

$$\text{LOGSIG (n)} = \frac{1}{1 + e^{-n}} \tag{12}$$

Table 3 represents the biases and weights for input-hidden and hidden-output layers.

The ANN model was validated using data consisting of the two end values (lowest and highest) of the entire range of input datasets. Outputs were predicted using the network. ANN-predicted and experimental values of ash rejection has been plotted in Figure 12. Similarly in **Figures SF1 and SF2** (supplementary file), comparison of predicted and experimental values of combustible recovery and separation efficiency respectively have been presented.

R, MAPE and MSE values observed in training, validation and testing stages of modeling have been given in Table 4.

R values were observed sufficiently close to 1. Hence, this ANN model can be used for the prediction of the output characteristics of present study with the fluidized bed separator. To check the performance of the ANN model, it has been compared with the results of a regression model. Regression model has been developed using a statistical software "Origin 8 (trial version)". To generate a multiple linear regression model, all the input and output data points were fed to the software. R values obtained from the analysis of datasets are 0.8812 (ash rejection), 0.6614 (combustible recovery) and 0.7828 (separation efficiency). These R values have been mentioned below in **Table ST2** (supplementary file) against the all R values obtained from the developed ANN model. It can be seen from the R values, that ANN model was able to predict the process performance better than the multiple linear regression model.

### *Sensitivity analysis*

Connection weight approach (CWA) and Garson's algorithm (GA) were used to determine the sensitivity of the outputs with respect to each operating variable. Order of significance of input parameters and interpretations for each output has been discussed. Equations used for calculating relative contribution of input parameters, as per "Garson's algorithm," are:[23,42–44]

$$\text{Cij} = \left(\frac{|X_{ij}|}{\sum_{i=1}^{N}|X_{ij}|}\right) \tag{13}$$

$$\text{Rik} = \frac{\sum_{j=1}^{M}\left(\left(\frac{|X_{ij}|}{\sum_{i=1}^{N}|X_{ij}|}\right)Y_{jk}\right)}{\sum_{i=1}^{N}\left(\sum_{j=1}^{M}\left(\left(\frac{|X_{ij}|}{\sum_{i=1}^{N}|X_{ij}|}\right)Y_{jk}\right)\right)} \tag{14}$$

By incorporating equation 13 in equation 14, the equation mentioned is obtained:

$$\text{Rik} = \frac{\sum_{j=1}^{M}(C_{ij}Y_{jk})}{\sum_{i=1}^{N}\left(\sum_{j=1}^{M}(C_{ij}Y_{jk})\right)} \tag{15}$$

Formulae used for calculating relative contribution of input parameters, as per "connection weight approach," are:[45]

$$\text{Siij} = \left(\frac{X_{ij}}{\sum_{i=1}^{N}X_{ij}}\right) \tag{16}$$

$$\text{Rik} = \frac{\sum_{j=1}^{M}\left(\left(\frac{X_{ij}}{\sum_{i=1}^{N}X_{ij}}\right)Y_{jk}\right)}{\sum_{i=1}^{N}\left(\sum_{j=1}^{M}\left(\left(\frac{X_{ij}}{\sum_{i=1}^{N}X_{ij}}\right)Y_{jk}\right)\right)} \tag{17}$$

By combining equations 16 & 17, the following equation was obtained:

Table 5. Relative contribution analysis for ash rejection, combustible recovery and separation efficiency.

| Output | Input parameters | Garson's algorithm (GA) | | Connection weight approach (CWA) | |
|---|---|---|---|---|---|
| | | Relative contribution, % | Ranking of input parameters | Si-value | Ranking of input parameters |
| Ash rejection | Feed size, μm | 27.1081 | 1 | −1.2780 | 2 |
| | Bed height, cm | 23.131 | 4 | −0.3317 | 4 |
| | Superficial velocity, cm/s | 24.0932 | 3 | 0.3321 | 3 |
| | Overflow tap height, cm | 24.6677 | 2 | 1.7786 | 1 |
| Combustible recovery | Feed size, μm | 27.0574 | 1 | −0.3457 | 4 |
| | Bed height, cm | 25.2178 | 2 | 1.1832 | 2 |
| | Superficial velocity, cm/s | 24.9239 | 3 | 0.3641 | 3 |
| | Overflow tap height, cm | 22.8008 | 4 | −2.4494 | 1 |
| Separation efficiency | Feed size, μm | 26.6183 | 2 | −3.4767 | 1 |
| | Bed height, cm | 28.292 | 1 | 1.5464 | 2 |
| | Superficial velocity, cm/s | 20.6325 | 4 | −0.4206 | 4 |
| | Overflow tap height, cm | 24.4572 | 3 | 0.6847 | 3 |

Table 6. Order of significance of input parameters as per GA, CWA and Taguchi methods.

| Output | Method | Order of significance |
|---|---|---|
| Ash rejection | GA | Feed size > Overflow tap height > Superficial velocity > Bed height |
| | CWA | Overflow tap height > Feed size > Superficial velocity > Bed height |
| | Taguchi-ANOVA | Overflow tap height > Feed size > Superficial velocity > Bed height |
| Combustible recovery | GA | Feed size > Bed height > Superficial velocity > Overflow tap height |
| | CWA | Overflow tap height > Bed height > Superficial velocity > Feed size |
| | Taguchi-ANOVA | Overflow tap height > Feed size > Superficial velocity > Bed height |
| Separation efficiency | GA | Bed height > Feed size > Overflow tap height > Superficial velocity |
| | CWA | Feed size > Bed height > Overflow tap height > Superficial velocity |
| | Taguchi-ANOVA | Feed size > Superficial velocity > Bed height > Overflow tap height |

$$\mathrm{Rik} = \frac{\sum_{j=1}^{M}\left(\mathrm{Si}_{ij}\mathrm{Y}_{jk}\right)}{\sum_{i=1}^{N}\left(\sum_{j=1}^{M}\left(\mathrm{Si}_{ij}\mathrm{Y}_{jk}\right)\right)} \tag{18}$$

where $X_{ij}$ is connection weight between the input neuron i and hidden neuron j, $Y_{jk}$ is connection weight between the hidden neuron j and output neuron k and $R_{ik}$ is percentage of the impact of the input variable $A_i$ on the output variable $B_k$. Relative contribution of inputs are calculated using corresponding absolute Si-values. Negative value of an input parameter suggests it will have an adverse influence on that particular output.[33,34,46] Si-values, relative contribution and ranking of each input parameter on all the outputs are mentioned in Table 5.

Order of significance of input parameters obtained for individual responses using Taguchi-ANOVA methodology and sensitivity analysis approaches are tabulated in Table 6.

Based on the results obtained from GA, feed size is the most important parameter for ash rejection with relative contribution 27.1081% and combustible recovery with relative contribution 27.0574%, whereas for separation efficiency with relative contribution 26.6183%, bed height was found to be the most significant parameter. As per the CWA results, overflow tap height is the most effecting parameter for ash rejection with Si-value of 1.7786 and combustible recovery with Si-value of −2.4494 and feed size, for separation efficiency with Si-value of −3.4767. Order of significance of input parameters obtained in connection weight approach (CWA) of sensitivity analysis for individual responses was found to be similar to the order of significance of input parameters obtained with statistical optimization using Taguchi-ANOVA method reported by Kumari et al.[12] Hence, CWA is considered better than GA for determining the order of significance of input parameters in this work.

## Conclusions

In this study, upgradation of low-grade coal was attempted through liquid-solid fluidization method and process was optimized by conducting several experimental runs at different set of operating conditions. Main purpose of the present paper was to develop an Indian coal specific model, which would help the coal washing operators in controlling the operating parameters. ANN is one of the very important modeling tool, which is used for continuous online controlling of the operating parameters in the plant conditions. Hence, the empirical model based on a three-layer (4:5:3) FFBP neural network was developed in the present study. It has been used for process modeling and response prediction of the liquid-solid fluidization system. Summarizing the significant points of this study as follows:

i. Bed characterization study is very significant for analyzing liquid-solid fluidization process and associated critical parameters. It was observed that pressure drop curves have variable slope in static bed region whereas bed expansion starts at the onset of fluidization inside the column. This can be attributed to that fact that the coal particles are not of mono-size, mono-density nature and have size distribution even in close size-ranges. It was used to determine the range of superficial velocity for all size-ranges and bed heights (packed and fluidized beds) to study the fluidization behavior of coal particles under study.
ii. Mathematical correlations used in this study assume particles are operating under certain conditions inside fluidization column. Comparison of experimental and predicted pressure drop and minimum fluidization

velocity values revealed that experimental values were closest to values predicted using Ergun's equation.

iii. Optimum result, with a maximum separation efficiency of 27.71%, was achieved at operating set of conditions of feed size-range: -1000 + 850 µm, bed height: 10 cm, superficial velocity: 3.54 cm/s and overflow tap height: 12 cm. Results were satisfactory for achieving certain ash rejection and thus liquid-solid fluidization technique can be suggested for coal cleaning and coal tailings utilization for the recovery of carbonaceous values.

iv. An artificial neural network model was developed using Levenberg-Marquardt method as training algorithm, LOGSIG as transfer function and MSE as performance function. All R values of 0.9960, 0.9952 and 0.9944 obtained for responses ash rejection, combustible recovery and separation efficiency respectively, suggest that predicted data are in agreement with target (experimental) data. Thus, the developed ANN model can be recommended for process modeling and performance analysis of liquid-solid fluidized bed separators.

v. Order of significance obtained from two methods of sensitivity analysis, Garson's algorithm and connection weight approach, show the variability in influence of input parameters for individual responses. Rankings obtained state that the order of significance of input parameters and the most sensitive parameter should be maintained more carefully to achieve superior performance of the fluidized bed separator followed in the given order.

Limitation of this study is that an empirical model is not applicable for general purpose and is suitable for specific cases. The model developed will only be suitable for Indian high ash and high NGM complex non-coking coal. The developed ANN architecture can then be extended for controlling the continuous liquid-solid fluidization systems. For doing that, the present ANN model has to be modified (small modification is required) to include the continuous training of ANN with the changing input data set. However, this is beyond the scope of the present manuscript for which industrial data from continuous liquid-solid fluidization system is required.

## Acknowledgement

Authors would like to express special appreciation and gratitude to Late Prof. Venugopal Rayasam for his valuable inputs in this study. Authors would also like to thank Department of Fuel, Minerals & Metallurgical Engineering, IIT (ISM) Dhanbad and Mineral Processing Department, CSIR-IMMT Bhubaneswar for providing all the research facilities.

## References

[1] Galvin, K. P.; Callen, A. M.; Spear, S. Gravity Separation of Coarse Particles Using the Reflux Classifier. Miner. Eng. **2010**, *23*, 339–349. DOI: 10.1016/j.mineng.2009.09.014.

[2] Tripathy, A.; Panda, L.; Sahoo, A. K.; Biswal, S. K.; Dwari, R. K.; Sahu, A. K. Statistical Optimization Study of Jigging Process on Beneficiation of Fine Size High Ash Indian Non-Coking Coal. Adv. Powder Technol. **2016**, *27*, 1219–1224. DOI: 10.1016/j.apt.2016.04.006.

[3] Ken, B. S.; Aich, S.; Saxena, V. K.; Nandi, B. K. Combustion Behavior of KOH Desulphurized Coals Assessed by TGA-DTG. *Energy Sources Part A* **2018**, *40*, 2458–2466. DOI: 10.1080/15567036.2018.1502844.

[4] Xu, Z.; Yoon, R. H. The Role of Hydrophobia Interactions in Coagulation. J. Colloid Interface Sci. **1989**, *132*, 532–541. DOI: 10.1016/0021-9797(89)90267-1.

[5] Das, M.; Meikap, B. C.; Saha, R. K. Study of Hydrodynamics and Dry Beneficiation Characteristics of Coal in the Riser of a Circulating Fluidized Bed Reactor. *Int. J. Coal Prep. Util.* **2013**, *33*, 266–276. DOI: 10.1080/19392699.2013.817394.

[6] Chaurasia, R. C.; Sahu, D.; Suresh, N. Cleaning of Coal by Multi Gravity Separator. Trans. Indian Inst. Met. **2018**, *71*, 1487–1495. DOI: 10.1007/s12666-018-1284-1.

[7] Richardson, J. F.; Zaki, W. N. Sedimentation and Fluidisation: Part I. *Trans. Inst. Chem. Eng.* **1979**, *32*, 35–53. DOI: 10.1016/S0263-8762(97)80006-8.

[8] Juma, A. K. A.; Richardson, J. F. Segregation and Mixing in Liquid Fluidized Beds. Chem. Eng. Sci. **1983**, *38*, 955–967. DOI: 10.1016/0009-2509(83)80016-5.

[9] Formisani, B.; Girimonte, R.; Longo, T. The Fluidization Process of Binary Mixtures of Solids: Development of the Approach Based on the Fluidization Velocity Interval. *Powder Technol.* **2008**, *185*, 97–108. DOI: 10.1016/j.powtec.2007.10.003.

[10] Galvin, K. P.; Walton, K.; Zhou, J. How to Elutriate Particles according to Their Density. Chem. Eng. Sci. **2009**, *64*, 2003–2010. DOI: 10.1016/j.ces.2009.01.031.

[11] Tripathy, A.; Bagchi, S.; Biswal, S. K.; Meikap, B. C. Effect of Fin Type Baffle on the Particle Hydrodynamics, Separation and Misplacement in a Liquid Solid Fluidized Bed Separator. Adv. Powder Technol. **2019**, *30*, 428–438. DOI: 10.1016/j.apt.2018.11.022.

[12] Kumari, A.; Tripathy, A.; Rayasam, V. Performance Characterization and Misplacement Studies of Liquid – Solid Fluidized Bed Density Separator for Coal Beneficiation Using Taguchi-ANOVA Method. Part. Sci. Technol. **2021**, *39*, 436–448. DOI: 10.1080/02726351.2020.1751357.

[13] Escudié, R.; Epstein, N.; Grace, J. R.; Bi, H. T. Effect of Particle Shape on Liquid-Fluidized Beds of Binary (and Ternary) Solids Mixtures: Segregation vs. mixing. Chem. Eng. Sci. **2006**, *61*, 1528–1539. DOI: 10.1016/j.ces.2005.08.028.

[14] Mawatari, Y.; Tatemoto, Y.; Noda, K. Prediction of Minimum Fluidization Velocity for Vibrated Fluidized Bed. *Powder Technol.* **2003**, *131*, 66–70. DOI: 10.1016/S0032-5910(02)00323-6.

[15] Mukherjee, A. K.; Kumar, A. Liquid/Solid Fluidization Its Role and Limitation in Fine beneficiation - A Review. Miner. Process. Extr. Metall. Rev. **2009**, *30*, 280–306. DOI: 10.1080/08827500902743916.

[16] Ham, J. M.; Thomas, S.; Guazzelli, E.; Homsy, G. M.; Anselmet, M. C. An Experimental Study of the Stability of Liquid-Fluidized Beds. Int. J. Multiphase Flow **1990**, *16*, 171–185. DOI: 10.1016/0301-9322(90)90052-K.

[17] Zenit, R.; Hunt, M. L. Solid Fraction Fluctuations in Solid-Liquid Flows. Int. J. Multiphase Flow **2000**, *26*, 763–781. DOI: 10.1016/S0301-9322(99)00066-X.

[18] Khosravi, B. H.; Basirat, T. H. Experimental Study on Hydrodynamic Characteristics of Gas-Solid Pulsed Fluidized Bed. *Powder Technol.* **2013**, *237*, 14–23. DOI: 10.1016/j.powtec.2013.01.001.

[19] Lim, K. S.; Zhu, J. X.; Grace, J. R. Hydrodynamics of Gas-Solid Fluidization. Int. J. Multiphase Flow **1995**, *21*, 141–193. DOI: 10.1016/0301-9322(95)00038-Y.

[20] Sahu, A. K.; Tripathy, A.; Biswal, S. K.; Parida, A. Stability Study of an Air Dense Medium Fluidized Bed Separator for Beneficiation of High-Ash Indian Coal. *Int. J. Coal Prep. Util.* **2011**, *31*, 127–148. DOI: 10.1080/19392699.2011.574936.

[21] Fan, X.; Zhang, G.; Zhao, Y.; Zhou, C.; Dong, L.; Duan, C. Effect of Middling Coal on Separation Efficiency in Air Dense

Gas–Solid Fluidized Bed. *Int. J. Coal Prep. Util.* **2018**, 1–17. DOI: 10.1080/19392699.2018.1498847.

[22] Olden, J. D.; Jackson, D. A. Illuminating the "'Black Box" ': A Randomization Approach for Understanding Variable Contributions in Artificial Neural Networks. *Ecol. Model.* **2002**, *154*, 135–150. DOI: 10.1016/S0304-3800(02)00064-9.

[23] Yadav, A. M.; Chaurasia, R. C.; Suresh, N.; Gajbhiye, P. Application of Artificial Neural Networks and Response Surface Methodology Approaches for the Prediction of Oil Agglomeration Process. *Fuel* **2018**, *220*, 826–836. DOI: 10.1016/j.fuel.2018.02.040.

[24] Tripathy, A.; Bagchi, S.; Biswal, S. K.; Meikap, B. C. Prediction of Degree of Particle Misplacement in Liquid Solid Fluidization Using Artificial Neural Network. Sep. Sci. Technol. **2020**, *55*, 68–80. DOI: 10.1080/01496395.2019.1565773.

[25] Asafa, T. B.; Tabet, N.; Said, S. A. M. Neurocomputing Taguchi Method – ANN Integration for Predictive Model of Intrinsic Stress in Hydrogenated Amorphous Silicon Film Deposited by Plasma Enhanced Chemical Vapour Deposition. *Neurocomputing* **2013**, *106*, 86–94. DOI: 10.1016/j.neucom.2012.10.019.

[26] Razzak, S. A.; Rahman, S. M.; Hossain, M. M.; Zhu, J. Investigation of Artificial Neural Network Methodology for Modeling of a Liquid – Solid Circulating Fluidized Bed Riser. *Powder Technol.* **2012**, *229*, 71–77. DOI: 10.1016/j.powtec.2012.06.010.

[27] Lourakis, M. I. A. A Brief Description of the Levenberg-Marquardt Algorithm Implemened by Levmar. *Found. Res. Technol.- Hellas (FORTH) GREECE.***2005**, 1-5.

[28] Gavin, H. P. The Levenburg-Marqurdt Algorithm for Nonlinear Least Squares Curve-Fitting Problems. *Duke University* **2020**, 1–19.

[29] Tripathy, A.; Bagchi, S.; Biswal, S. K.; Meikap, B. C. Study of Particle Hydrodynamics and Misplacement in Liquid–Solid Fluidized Bed Separator. Chem. Eng. Res. Des. **2017**, *117*, 520–532. DOI: 10.1016/j.cherd.2016.11.009.

[30] Panda, L.; Banerjee, P. K.; Biswal, S. K.; Venugopal, R.; Mandre, N. R. Artificial Neural Network Approach to Assess Selective Flocculation on Hematite and Kaolinite. Int. J. Miner. Metall. Mater. **2014**, *21*, 637–646. DOI: 10.1007/s12613-014-0952-3.

[31] Panda, L.; Sahoo, A. K.; Tripathy, A.; Biswal, S. K.; Sahu, A. K. Application of Artificial Neural Network to Study the Performance of Jig for Beneficiation of Non-Coking Coal. *Fuel* **2012**, *97*, 151–156. DOI: 10.1016/j.fuel.2012.02.018.

[32] Chaurasia, R. C.; Nikkam, S. Application of Artificial Neural Network to Study the Performance of Multi Gravity Separator (MGS) Treating Iron Ore Fines. Part. Sci. Technol. **2017**, *35*, 93–102. DOI: 10.1080/02726351.2015.1131791.

[33] Wang, L.; Sharifzadeh, M.; Templer, R.; Murphy, R. J. Bioethanol Production from Various Waste Papers : Economic Feasibility and Sensitivity Analysis. Appl. Energy **2013**, *111*, 1172–1182. DOI: 10.1016/j.apenergy.2012.08.048.

[34] Pianosi, F.; Beven, K.; Freer, J.; Hall, J. W.; Rougier, J.; Stephenson, D. B.; Wagener, T. Environmental Modeling & Software Sensitivity Analysis of Environmental Models : A Systematic Review with Practical Work Flow. *Environ. Model. Software* **2016**, *79*, 214–232. DOI: 10.1016/j.envsoft.2016.02.008.

[35] Olden, J. D.; Joy, M. K.; Death, R. G. An Accurate Comparison of Methods for Quantifying Variable Importance in Artificial Neural Networks Using Simulated Data. *Ecol. Model.* **2004**, *178*, 389–397. DOI: 10.1016/j.ecolmodel.2004.03.013.

[36] Gevrin, F.; Masbernat, O.; Simonin, O. Granular Pressure and Particle Velocity Fluctuations Prediction in Liquid Fluidized Beds. Chem. Eng. Sci. **2008**, *63*, 2450–2464. DOI: 10.1016/j.ces.2008.01.031.

[37] Daleffe, R. V.; Ferreira, M. C.; Freire, J. T. Effects of Binary Particle Size Distribution on the Fluid Dynamic Behaviour of Fluidized, Vibrated and Vibrofluidized Beds. *Braz. J. Chem. Eng.* **2008**, *25*, 83–94. DOI: 10.1590/S0104-66322008000100010.

[38] Ergun, S.; Orning, A. A. Fluid Flow through Randomly Packed Columns and Fluidized Beds. *Ind. Eng. Chem.* **1949**, *41*, 1179–1184. DOI: 10.1021/ie50474a011.

[39] Carman, P. C. Fluid Flow through Granular Beds. *Trans. Inst. Chem. Eng.* **1937**, *15*, S32–S48. DOI: 10.1016/s0263-8762(97)80003-2.

[40] Wen, C. Y.; Yu, Y. H. A Generalized Method for Predicting the Minimum Fluidization Velocity. *AIChE J.* **1966**, *12*, 610–612. DOI: 10.1002/aic.690120343.

[41] Mohanta, S.; Meikap, B. C. Influence of Medium Particle Size on the Separation Performance of an Air Dense Medium Fluidized Bed Separator for Coal Cleaning. *J. S Afr. Inst. Min. Metall.* **2015**, *115*, 661–766. DOI: 10.17159/2411-9717/2015/v115n8a13.

[42] Sahu, D.; Chaurasia, R. C.; Suresh, N. Statistical Studies on High Ash Indian Coal Crushed to (− 3 mm) Using 76 mm Dense Medium Cyclone. *Int. J. Coal Prep. Util.* **2019**, 1–21. DOI: 10.1080/19392699.2019.1605987.

[43] Garson, G. D. Interpreting Neural Network Connection Weights. *AI Expert* **1991**, *6*, 46–51. DOI: https://dl.acm.org/doi/10.5555/129449.129452.

[44] Chaurasia, R. C.; Sahu, D.; Suresh, N. Prediction of Ash Content and Yield Percent of Clean Coal in Multi Gravity Separator Using Artificial Neural Networks. *Int. J. Coal Prep. Util.* **2021**, *41*, 362–369. DOI: 10.1080/19392699.2018.1547282.

[45] Cao, M.; Qiao, P. Neural Network Committee-Based Sensitivity Analysis Strategy for Geotechnical Engineering Problems. *Neural Comput. Appl.* **2008**, *17*, 509–519. DOI: 10.1007/s00521-007-0143-5.

[46] Ross, C. F.; Patel, B. A.; Slice, D. E.; Strait, D. S.; Dechow, P. C.; Richmond, B. G.; Spencer, M. A. Modeling Masticatory Muscle Force in Finite Element Analysis : Sensitivity Analysis Using Principal Coordinates analysis. *Anat. Rec. Part A* **2005**, *283*, 288–299. DOI: 10.1002/ar.a.20170.